TISSUE ENGINEERING: Part C
Volume 17, Number 3, 2011

DOI: 10.1089/ten.tec.2010.0399

Isolation, Characterization, and Expansion Methods for Defined Primary Renal Cell Populations from Rodent, Canine, and Human Normal and Diseased Kidneys

Sharon C. Presnell, Ph.D., Andrew T. Bruce, B.S., Shay M. Wallace, B.A., Sumana Choudhury, M.S., Christopher W. Genheimer, B.S., Bryan Cox, B.S., Kelly Guthrie, B.S., Eric S. Werdin, B.S., Patricia Tatsumi-Ficht, B.S., Roger M. Ilagan, Ph.D., Russell W. Kelley, Ph.D., Elias A. Rivera, M.H.S., John W. Ludlow, Ph.D., Belinda J. Wagner, Ph.D., Manuel J. Jayo, D.V.M., Ph.D., and Timothy A. Bertram, D.V.M., Ph.D.

Chronic kidney disease (CKD) is a global health problem; the growing gap between the number of patients awaiting transplant and organs actually transplanted highlights the need for new treatments to restore renal function. Regenerative medicine is a promising approach from which treatments for organ-level disorders (e.g., neurogenic bladder) have emerged and translated to clinics. Regenerative templates, composed of biodegradable material and autologous cells, isolated and expanded *ex vivo*, stimulate native-like organ tissue regeneration after implantation. A critical step for extending this strategy from bladder to kidney is the ability to isolate, characterize, and expand functional renal cells with therapeutic potential from diseased tissue. In this study, we developed methods that yield distinct subpopulations of primary kidney cells that are compatible with process development and scale-up. These methods were translated to rodent, large mammal, and human kidneys, and then to rodent and human tissues with advanced CKD. Comparative *in vitro* studies demonstrated that phenotype and key functional attributes were retained consistently in *ex vivo* cultures regardless of species or disease state, suggesting that autologous sourcing of cells that contribute to *in situ* kidney regeneration after injury is feasible, even with biopsies from patients with advanced CKD.

Introduction

The prevalence of chronic kidney disease (CKD) is rising rapidly, increasing >33% between 1996 and 2006.[1] CKD is frequently secondary to hypertension and type 2 diabetes, two diseases with rising prevalence. Although pharmacological interventions that address primary dysfunctions can slow progression of kidney damage and disease, dialysis or whole organ transplantation is ultimately required to achieve sufficient renal filtration to sustain life. Currently, >500,000 people in the United States require dialysis or a kidney transplant to survive, accounting for >$22 billion annually in Medicare costs (6% of the total Medicare budget).[2]

Kidney transplantation is the definitive standard of care for CKD, providing better long-term survival[3] and cost-effectiveness[4] than dialysis; however, there is a chronic shortage of organs. Despite increases in both cadaveric and living kidney donors, the rate of transplantation per 100 dialysis patient-years in the United States is actually decreasing.[5] These realities underscore the need for new treatment paradigms that can alleviate some of the healthcare burden imposed by dialysis and transplant by providing substantial and durable augmentation of kidney functions to slow progression of CKD. Regenerative medicine technologies hold promise for providing next-generation therapeutic options for CKD, especially if they can be initiated effectively after the onset of progressive disease.

Regenerative medicine approaches that combine autologous cells derived from the target organ (also known as an "autologous/homologous cell sourcing strategy"[6]) with biomaterials have transitioned to clinical trials designed to augment bladder, a tubular organ.[7,8] We sought to investigate the feasibility of applying a similar strategy to kidney, a solid organ, in the experiments reported here. The choice of unfractionated primary kidney cells (UNFX)[9,10] as a starting population was based on literature support of the therapeutic potential for augmenting renal function in the context of CKD when administered after the onset of disease. In a rodent model, chronic renal disease was established by heminephrectomy and ischemia to the intact kidney.[11] Injection of a heterogeneous mixture of human fetal kidney cells,

Portions of this data appeared in an abstract published from the Experimental Biology 2009 meeting.
Tengion Laboratories, Department of Science and Technology, Winston-Salem, North Carolina.

containing embryonic tubular cells, via the vena cava into rats with established disease led to transient improvement of all functional parameters. The recovery observed in rats receiving fetal kidney cells was more rapid in the context of chronic disease state than that observed in rats receiving bone marrow-derived mesenchymal stem cells. When acute damage was superimposed in the model, the fetal kidney cells showed therapeutic benefit at a level equivalent to that observed with bone marrow-derived mesenchymal stem cells.

One subpopulation of renal cells that has been repeatedly associated with restoring renal function after acute renal injury in both preclinical and clinical studies is tubular cells. After acute injury, resident, surviving tubular cells dedifferentiate and proliferate to replace the lost cells throughout the nephron.[12] In a series of experiments designed to assess the effects of transplanted bone marrow cells in restoring renal function in a model of chronic renal injury that leveraged genetic tools for discerning resident from transplanted cells, resident tubular cells were observed to be key participants in the recovery process.[13–15] Finally, phase II clinical trials of an extracorporeal renal tubule assist device, which combined a bioreactor containing living proximal tubular cells with conventional hemodialysis, demonstrated that the bioreactor-augmented dialysis procedure conferred a significant survival benefit and more rapid restoration of kidney function in patients with acute renal failure.[16]

An autologous/homologous cell sourcing strategy for developing cellular components of candidate therapies for CKD could be considered feasible if methods for isolating, characterizing, and expanding (ICE methods) defined renal cell populations that had the potential for conferring therapeutic benefit could be designed and applied to disease-relevant animal models and humans.[6] Of particular relevance to feasibility are ICE methods that yield target cell populations from patients with CKD using a clinically relevant tissue harvesting procedure. Developing these ICE methods for UNFX and a tubule-enriched subpopulation and applying them to rodent, canine, and human tissues was the goal of this study. Additionally, we limited our evaluation to protocols that are compatible with process development and scale-up.

Healthy canine and human kidney tissue samples were used to demonstrate that ICE methods yielding rodent UNFX and B2, a tubule-enriched subpopulation of UNFX, could be adapted successfully to a relevant preclinical species (dog) and the clinically relevant human. Proof of principle for isolation and expansion of UNFX and generation of B2, a tubule-enriched subpopulation of UNFX, from diseased kidney tissue was achieved in the ZSF1 (*fa*/*fa*^{cp}) rat model, which is a metabolic disease model characterized by overt and progressive kidney disease secondary to obesity and type 2 diabetes.[17] Finally, whole kidney tissue was collected from five human organ donors with advanced CKD to demonstrate that functional B2 cells were present in the tissue and could be isolated and propagated successfully, even from small needle core biopsies. The data presented herein provide evidence that an autologous/homologous cell sourcing strategy for UNFX and B2 renal cell populations is translatable to large mammals and to humans with CKD, thus supporting the feasibility of these ICE methods for obtaining defined renal cell populations with potential for conferring therapeutic benefit in the treatment of CKD.

Materials and Methods

Tissue sourcing

Lewis and ZSF1 tissues were sourced from Charles Rivers Laboratories and canine tissue from the Integra Group in compliance with policies governing the use of laboratory animals. With the exception of HK023, human tissue was sourced through the National Disease Research Institute in compliance with policies governing the use of human tissues for research. Human specimen HK023 was obtained as biopsy material under informed consent with approval from the Institutional Review Board of the University of North Carolina at Chapel Hill.

Cell isolation, culture, and separation

Unfractionated heterogeneous primary renal cell cultures (UNFX) were established and maintained as described for all species.[9,10] For human samples initiated from biopsy, 2 mm core biopsies (0.02 g tissue) were collected with an Easy Core™ Biopsy System (Boston Scientific) and washed 2 × in Hanks balanced salt solution (without magnesium chloride–$MgCl_2$–and calcium chloride–$CaCl_2$), minced, and digested for 30 min in Dispase (Stem Cell Technologies) containing 300 U of collagenase type IV (Worthington Biochemical Corporation) and 5 mM calcium chloride (Sigma). Cells were cultured in 35 mm tissue culture dishes (Corning/Costar). Cell yields were determined by counting viable cells at passage and growth rates were calculated as ln(fold increase)/time. Population doubling times were calculated as ln(2)/growth rate.

Cell subpopulations from dog and human were obtained from UNFX cultures that were placed into low-oxygen (2%) conditions for 24 h before harvest via trypsin, which facilitates the subsequent distribution of cell subpopulations and enhances specific phenotypic attributes (unpublished observations). Two-milliliter suspensions of 60–75 × 10^6 UNFX cells were loaded onto four-step iodixanol (OptiPrep; 60% w/v in unsupplemented Keratinocyte Serum Free Media; Invitrogen) density gradients layered specifically for rodent (16%, 13%, 11%, and 7%), canine (16%, 11%, 10%, and 7%), or human (16%, 11%, 9%, and 7%). Gradients were centrifuged at 800*g* for 20 min at room temperature (without brake). Bands of interest were removed via pipette and washed 2 × in sterile phosphate-buffered saline (PBS).

Gene expression analysis

RNA isolation and cDNA preparation. Tissue or cell samples were homogenized using the QIAshredder (Cat #79656; Qiagen) and RNA was isolated using an RNeasy Plus Mini isolation kit (Cat # 74134; Qiagen). RNA integrity was verified and samples were quantified via spectrophotometric analysis.[18] cDNA was synthesized using the Superscript® Vilo cDNA synthesis kit (Cat# 11754-250; Invitrogen).

Quantitative reverse transcriptase-polymerase chain reaction assays. Expression of erythropoietin (*EPO*), E-cadherin (*ECAD*), N-cadherin (*NCAD*), cubilin, 1 alpha, 25-dihydroxyvitamin D3-24-hyroxylase (*CYP24*), aquaporin-2 (*AQP2*), nephrin (*NEPH*), vascular endothelial growth factor, and CD31 (*PECAM*) were examined via quantitative

real-time polymerase chain reaction (PCR) using TaqMan Gene Expression Master Mix (Cat #4369016), catalogued TaqMan probes and primer sets (Table 1) from Applied Biosystems, and an ABI-Prism 7300 Real-time PCR System.

Determination of relative quantification values. Relative quantification values were calculated according to manufacturer's protocols by 7300 System SDS Software version 1.4.0.25 (Applied Biosystems). Gene expression in UNFX cultures was quantified relative to cDNA amplified from peptidylprolyl isomerase B (for rodent genes), TATA binding protein (for canine genes), or peptidylprolyl isomerase A (*PPIA*) (for human genes). Gene expression in B2 and B4 subpopulations was quantified relative to the same cDNA amplified from a sample of the corresponding UNFX input culture used to generate the subpopulations. Reproducibility of B2 gene expression patterns among human tissue biopsies was measured as the fold change in expression of target genes in comparison to endogenous control (*PPIA*). Briefly, fold change cycle threshold (Ct) values of samples were generated by 7300 System SDS Software version 1.4.0.25 An average Ct value for the endogenous control (*PPIA*) was calculated for B2 samples across all plates. ΔCT for B2 target genes was calculated as Ct(target gene) – AvgCt(endogenous). Fold change for the samples was calculated as $2^{-\Delta Ct}$.

Flow cytometry

Phenotypic characterization of UNFX and B2 cells isolated from rodent, canine, and human tissues was performed by standard flow cytometric methods[19] on a FACS Aria (Becton Dickinson). Data were analyzed with FlowJo (Tree Star) software. Primary antibodies (used at 1 μg/mL) and isotype-matched controls (used at 1 μg/mL) are listed in Table 2. Briefly, cells fixed in 2% paraformaldehyde were washed 2× in sterile PBS and stained with primary antibodies at a concentration of 1 μg/10^6 cells/mL and incubated for 2 h at 4°C. After incubation with primary antibody the cells were washed 2× and stained with secondary antibody at a concentration of 1 μg/10^6 cells/mL and incubated for 30 min at room temperature protected from light. After incubation the cells were washed 2× and subjected to flow cytometry.

Albumin uptake assay

Renal proximal tubular cell function was assessed by the activation and inhibition of albumin endocytosis mediated by specific proximal tubule receptors, megalin and cubilin, as described.[20] Cultures were grown to confluence (7–10 days) and assayed 1–2 days post-confluence. Eighteen to 24 h before assay initiation, the growth medium was replaced with assay buffer consisting of serum-free, phenol red-free, low-glucose (1 g/L) Dulbecco's modified Eagle's medium containing 2 mM glutamine, 10 mM HEPES [4-(2-hydroxyethyl)-1-piperazineethanesulfonic acid] buffer (all from Invitrogen). On the day of assay, cells were washed twice with assay buffer consisting 1.8 mM $CaCl_2$ and 1 mM $MgCl_2$, and incubated with assay buffer for 30 min in a humidified chamber at 37°C/5% CO_2 (carbon dioxide) to ensure adequate exposure to cofactors. Cells were then exposed to a final concentration of 10–30 μg/mL rhodamine-conjugated human albumin (ALB-*RHO*) (Abcam, Inc.) for 30 min at 37°C/5% CO_2. Wells were washed three times with ice cold PBS to stop endocytosis and fixed immediately with 2% paraformaldehyde containing 10 μg/mL Hoechst nuclear dye (Invitrogen). Addition of 1 μM receptor-associated protein (recombinant human; Innovative Research™), a specific competitive inhibitor of megalin:cubilin-mediated albumin uptake[20] in control cultures served to demonstrate specificity of the reaction. Inducibility of ALB-*RHO* endocytosis was examined by pretreatment of UNFX cultures with 10^{-8} M human angiotensin II (Sigma-Aldrich) for 4 h before exposure to ALB-*RHO*, as described.[21] Cells were observed and images captured via microscopy using a BD Pathway 855 High-Content BioImager (Becton Dickinson) and quantitative image analysis was conducted with IN Cell Investigator software with Multi-Target Analysis Module (GE Healthcare).

Measurement of hydrolase activity

Enzymatic activity of two proximal tubule-associated hydrolases, gamma glutamyl transpeptidase (GGT or *GGT1* for the gene product) and leucine aminopeptidase (LAP), was measured in human UNFX cultures at passage 1. Established cultures were trypsinized and replated at 4000 cells/cm^2 and maintained in standard growth conditions for 7 days before assay. The GGT assay was adapted from published methods.[22] Briefly, wells were washed and 0.5 mL of substrate reagent

Table 1. TaqMan Probes Used

Gene	*Rat TaqMan assay*	*Canine TaqMan assay*	*Human TaqMan assay*
Erythropoietin (EPO)	Rn01481376_m1	Cf02626689_g1	Hs01071097_m1
E-cadherin (ECAD)	Rn00580109_m1	Cf02624269_m1	Hs00170423_m1
N-Cadherin (NCAD)	n/a	n/a	Hs00169953_m1
Cubilin (CUB)	Rn00584200_m1	Cf02695209_m1	Hs00153607_m1
Vitamin D hydroxylase (CYP24)	n/a	n/a	Hs01379776_m1
Aquaporin-2 (AQP2)	n/a	n/a	Hs00166640_m1
Nephrin (NEPH)	Rn00575235_m1	Cf02703355_m1	Hs00190446_m1
Vascular endothelial growth factor	n/a	Cf02623449_m1	Hs00900055_m1
PECAM (CD31)	Rn01467262_m1	Cf02659338_m1	Hs00169777_m1
Peptidylprolyl isomerase B	Rn00574762_m1	n/a	n/a
Peptidylprolyl isomerase A	n/a	n/a	Hs00000004_m1
TATA binding protein	n/a	Hs99999910_m1	n/a

n/a, not applicable.

Table 2. Antibodies for Flow Cytometry

Protein/species/isotype	*Manufacturer (catalog no.)*
CK8/18/19/ms/IgG1	Abcam (ab41825)
E-Cadherin/ms/IgG2a	BD Biosciences (610182)
Pan-Cadherin/rb/IgG	Abcam (ab6528)
GGT-1/rb/IgG	Santa Cruz (sc-20638)
Aquaporin 2/rb/IgG	Abcam (ab64154)
CD31/ms anti-human/IgG1	BD Biosciences (555444)
CD31/ms anti-rat/IgG1	BD Biosciences (555025)
CD146/ms/IgG1	Abcam (ab24577)
Ms IgG1 Isotype control	DAKO (X0931)
Ms IgG2a Isotype control	DAKO (X0932)
Rb IgG Isotype control	Invitrogen (021202)
Goat anti-ms IgG1 A488	Invitrogen (A21121)
Goat anti-ms IgG2a A488	Invitrogen (A21131)
Chicken anti-rb IgG A488	Invitrogen (A21441)

GGT, gamma glutamyl transpeptidase; ms, mouse; rb, rabbit.

comprised of 2.5 mM *L*-glutamic acid γ-p-nitroanilide (Sigma) in Tris-HCl (pH 8.6) containing 150 mM NaCl and 50 mM glycylglycine was added for 1 h at room temperature. GGT activity was calculated as mean absorbance at 405 nm (corrected with reagent blank) of triplicate samples. Leucine aminopeptidase activity was determined in a similar assay using 3 mM *L*-leucine p-nitroanilide in PBS as substrate reagent. LLC-PK1 cell lysates (ATCC) served as positive controls.[23]

Isoelectric focusing and western blotting for detection of EPO

Frozen whole kidney tissue from human kidneys HK16, HK17, HK18, HK19, HK20, and HK21 was used for protein sample collection. All tissues were lysed for 15 min at room temperature in a buffer consisting of 50 mM Tris (pH 8.0), 120 mM NaCl, 0.5% NP40, and protease inhibitor cocktail (Roche Applied Science) with rocking followed by centrifugation for 10 min at 13,000 RPM. Protein concentrations were determined from supernatants by Bradford Assay.[18] Lysate prepared from cultured human foreskin fibroblasts served as a negative control. Proteins in each sample were separated by isoelectric focusing (IEF) by adding 40 μg of protein per well to pH 3–10 IEF Gels (Invitrogen). Colorimetric IEF marker protein standards (10 μg/lane; Serva Electrophoresis; Cat# 39212) were loaded in two lanes, one on either side of the sample lanes. The gels were electrophoresed for 1 h at 100 V followed by 1 h at 200 V and finally 30 min at 500 V in pH 3–10 cathode and anode buffer (Invitrogen). The proteins were then transferred to a nitrocellulose membrane using the I-Blot system (Invitrogen) following the manufacturer's instructions. Transfer quality was assessed visually on the membrane using the colorimetric standard bands at pH 4.5, 4.2, and 3.5 (Epo protein runs at pH 4.2). After transfer, the membrane was blocked with 15 mL of 4% w/v low-fat milk dissolved in Tris Buffered Saline with 0.1% Tween-20 (TBS-T) (Sigma) for 2 h at room temperature with rocking. The membrane was probed overnight at room temperature with anti-human EPO monoclonal IgG_{2a} MAb 2871 (R&D Systems) at a 1:600 dilution in 5 mL TBS-T with 2% w/v low-fat milk. The membrane was washed three times for 10 min each wash with TBS-T, and then probed with an horseradish peroxidase-conjugated rabbit anti-mouse IgG (Zymed) at a 1:50,000 dilution (within manufacturer's recommended range for detection with ECL Advanced Chemiluminescent reagent) in TBS-T with 2% w/v low-fat milk for 1.5 h at room temperature with rocking. The membrane was washed three times for 10 min each wash in TBS-T, followed by two 10-min washes in deionized water. The blot was developed using ECL Advance chemiluminescent reagent (GE Healthcare) following the manufacturer's instructions.

Renal histology

Representative kidney samples were collected and placed in 10% buffer formalin for 24 h. Sections were dehydrated in ascending grades of ethanol and embedded in paraffin. Paraffin blocks were cut at 5-μm thick sections, mounted on charged slides and processed for hematoxylin and eosin, Masson's trichrome and Periodic Acid Schiff staining (PAS) in accordance with standard staining protocols.[24] Digital microphotographs were captured at total magnification of ×40, ×100, and ×400 using a Nikon Eclipse 50i microscope fitted with a Digital Sight (DS-U1) camera. Renal morphology changes were assessed adopting commonly used[25] severity grade schemes (grades 1, 2, 3, and 4), to which descriptive terms (minimal, mild, moderate, and marked/severe) are applied to determine the degree of glomerulosclerosis, tubular atrophy and dilatation, tubular casts, and interstitial fibrosis and inflammation.

Statistical analyses

Basic statistics were calculated using Excel 2003 (Microsoft Corporation).

Table 3. UNFX Isolation and Characterization from Rodents, Canines, and Humans

	UNFX yield and flow characterization		
	Lewis rat	*Canine*	*Human*
Viable cells obtained from tissue [(cells/gm) × 10^6]	194 ± 57 ($n = 25$)	72 ± 40 ($n = 16$)	26 ± 24 ($n = 3$)
CK8/18/19+ (epithelial)	86.8%	86.8%	95.4%
GGT1+ (tubular)	41.3%	54.5%	24.8%
AQP2+ (ductular)	43.6%	47.4%	16.1%

Tissue was sourced from Lewis rat, canine (mongrel) >6 months old, and human whole kidney samples and UNFX cells were isolated. Cell yields were determined at primary isolation and normalized to gram of tissue based on the wet weight of tissue processed. Relative percentages of epithelial (CK8/18/19+), tubular (GGT1+), ductular (AQP2+), and vascular (PECAM+/CD146+) cells were measured by flow cytometry of primary (Lewis rat and canine) or passage 2 (human) UNFX cultures.

UNFX, unfractionated primary kidney cells.

Results

UNFX composition in normal rodent, canine, and human kidneys

UNFX is a heterogeneous mixture of renal cells isolated from the cortical and medullary zones. UNFX isolates contain cells from major compartments of the kidney and retain functional attributes (e.g., bioresponsive erythropoietin expression, receptor-mediated albumin uptake, and the ability to recapitulate renal structures in three-dimensional culture).[9,10,26] Flow cytometric analyses of representative cultures demonstrated that UNFX isolates from rodent, canine, and human normal kidneys were composed predominantly of CK8/18/19(+) epithelial cells and contained significant numbers of *GGT*(+) tubular cells and *AQP2*(+) ductular cells (Table 3). Although initial yields of UNFX from human were lower than those observed from rodent and dog, cultures were established successfully from 3/3 human donors and had a predominantly epithelial phenotype (Table 3). Human and dog UNFX cultures had fewer nonepithelial cells (CK8/18/19-negative) than rodent UNFX and cultures derived from all species contained small proportions (<5%) of endocrine, vascular, and glomerular cells as well as some undefined cell types (data not shown).

A

	UNFX subpopulation			
	B2		*B4*	
	Density (g/mL)	*% of UNFX*	*Density (g/mL)*	*% of UNFX*
Lewis rat ($n=12$)	1.045–1.063	67.0 ± 22.3	1.073–1.091	1.22 ± 0.28
Canine ($n=8$)	1.045–1.058	70.0 ± 10.0	1.063–1.091	1.5 ± 0.8
Human ($n=1$)	1.045–1.052	49.0%	1.063–1.091	2.7%

B

	B2 flow characterization (% positive)		
	Lewis rat	*Canine*	*Human*
Samples assayed	5	4	2
ECAD	97.3 ± 1.2	nd	99.1 ± 06
Pan-Cadherin	nd	92.4 ± 1.2	nd
CK8/18/19	83.5 ± 0.7	87.5 ± 0.2	99.0 ± 0.3
GGT1	52.1 ± 5.7	77.3 ± 4.3[a]	51.5 ± 4.0
AQP2	48.2 ± 5.4	42.1 ± 5.4	41.1[b]
PECAM (CD31)	1.41 ± 0.2	nd	<1%
CD146	nd	2.8 ± 0.4	nd

[a] $n=2$.
[b] $n=1$.
nd, not determined.

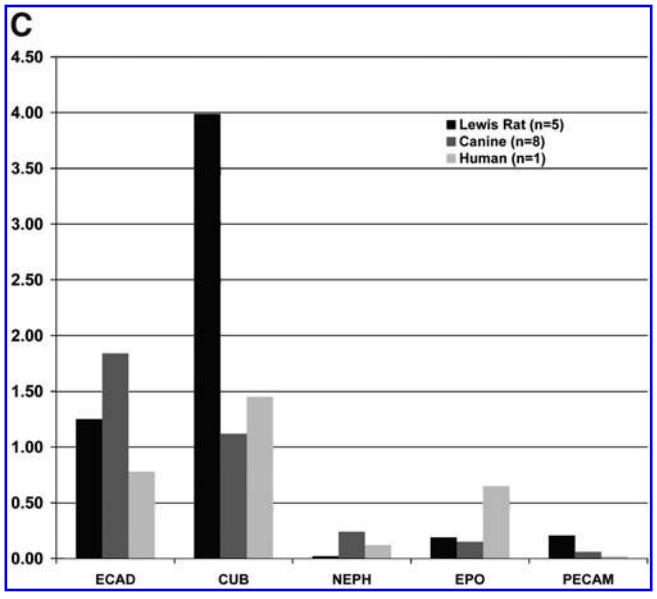

Isolation of defined subpopulations from established cultures of UNFX

Iodixanol gradients are used in the processing of primary autologous cells for clinical trials.[7,8,27] Four-step density gradients, optimized for each species, separated UNFX cells into five subpopulations, designated B1 to B5. Detailed gene array analysis of rodent cells revealed that the B2 subpopulation was enriched for tubular epithelial cells (see Supplementary Data available online at www.liebertonline.com/ten). On the basis of the tubular cell enrichment achieved by iodixanol density gradient centrifugation, the high proportion of UNFX represented by B2, and previous work identifying tubular cells as key participants in renal regeneration, we focused on this subpopulation for translating ICE methods to canine and human normal kidneys. The B4 subpopulation was used as a tubule-depleted comparator. Isolation parameters and yield percentage relative to UNFX for B2 and B4 subpopulations are shown in Figure 1A.

Five markers were selected to characterize B2 subpopulations by flow cytometric analysis of protein expression (Fig. 1B) and gene expression relative to the tubule-depleted B4 fraction by quantitative reverse transcriptase (RT)-PCR (Fig. 1C): E-cadherin, CK8/18/19, *GGT1* (protein only), *AQP2*, *PECAM* (CD31), and *NEPH* (gene expression only). For protein expression in canine tissues, substitute antibodies used for flow cytometric analysis were a pan-cadherin antibody, E-cadherin, and a CD146 antibody for PECAM.

FIG. 1. B2 and B4 subpopulations were generated from UNFX cultures derived from Lewis rat (passage 0), canine (passage 0), and human (passage 2) kidneys. Reported for each species are **(A)** the buoyant density range (g/mL) of iodixanol required to generate B2 and B4, and the relative proportion of UNFX that B2 and B4 represent; **(B)** quantitative flow-cytometric population analysis examining epithelial (*ECAD*/CK8/18/19/PAN-Cadherin), tubular (gamma glutamyl transpeptidase 1 [*GGT1*]), ductular (aquaporin-2 [*AQP2*]), and vascular (*PECAM*/CD146) marker expression of the B2 subpopulation; and **(C)** quantitative reverse transcriptase-polymerase chain reaction (qRT-PCR) gene expression analysis of B2, expressed relative to B4, for epithelial marker E-Cadherin (*ECAD*), tubular marker Cubilin (*CUB*), glomerular marker nephrin (*NEPH*), endocrine marker erythropoietin (*EPO*), and vascular marker *PECAM*.

These characterization profiles were used to translate ICE methods to diseased tissues from rodents and humans with established CKD. Comparative gene expression analyses of B2 and B4 among samples confirmed the epithelial/tubular nature of B2 from rodent, dog, and human, and confirmed the segregation of vascular, *EPO*-expressing, and glomerular cells to B4 (Fig. 1C). The selected B2 subpopulation was more homogeneous than UNFX. The relative proportion of epithelial cells (i.e., *ECAD*+, Pan-Cadherin+, or CK8/18/19+) was increased to >90% in B2 across species, but the most notable distinction between UNFX and B2 was the enrichment in B2 of the proportion of *GGT1*+ tubular cells—ranging from a 1.4-fold increase in the dog to >2.0-fold increase in the human (compare Table 3 with Fig. 1B).

UNFX and B2 cells from diseased rodent kidneys

Obese ZSF1 (*fa*/*fa*^{cp}) rats develop CKD by 8 weeks of age, whereas lean ZSF1 rats retain near normal renal structure (Fig. 2A) and function.[17,28–30] UNFX cell suspensions were prepared from 10 to 35-week-old obese and lean ZSF1 rats (Fig. 2B) and subpopulations B2 and B4 isolated (Fig. 2C). Of note was the reduction in the B4 component in ZSF1/obese UNFX cultures (0.5%) compared to ZSF1/lean (3.1%). The resulting B2 subpopulation profiles (Fig. 2D, E) also showed some variability (consistent with the reduction in B4) but demonstrated that B2 from ZSF1/obese diseased tissue was a predominantly tubular epithelial population with characteristics similar to B2 isolated from ZSF1/lean kidneys.

UNFX and B2 cells from humans with CKD

Eight human kidneys were obtained via approved organ procurement procedures (Fig. 3A): three from patients without CKD and five from patients with CKD. Renal disease was confirmed by serum chemistry at tissue harvest and histopathology (HK18 tissue in Fig. 3B; histopathology of all CKD samples available online as Supplementary Data). Severity of CKD in human patients varied, but without exception all human CKD patients were characterized by significant elevations in blood urea nitrogen (BUN) and serum creatinine (sCREAT) and were either anuric or had significant proteinuria.

Isolation and functional characterization of UNFX from human CKD kidneys

Initial cell yields per gram of tissue were lower from CKD (Table 4), which was anticipated from ZSF1 results (Fig. 2B). Without exception, application of the ICE methods developed for normal human tissue (Table 3) to human CKD tissues (5/5) yielded UNFX cultures that could be passaged, cryopreserved, and used to generate the B2 subpopulation (Table 4). To evaluate the functional status of UNFX isolates from human CKD tissues, oxygen regulation of *EPO* expression and receptor-mediated albumin uptake was assayed because previous studies of rodent UNFX demonstrated that oxygen-regulated *EPO*-producing endocrine cells and albumin-transporting tubular cells were retained in UNFX.[9,26] *EPO* protein was assayed by western blot analysis and *EPO* levels in CKD-derived kidney tissues were comparable or greater than in non-CKD tissues (Fig. 4A), indicating that *EPO*-producing activity was intact in the CKD kidneys despite systemic anemia. To assess the continued expression and oxygen-responsiveness of *EPO*, one group of human UNFX cultures was subjected to a hypoxic stimulus and the levels *EPO* mRNA in 21% and 2% O_2 were quantified by RT-PCR. *EPO* mRNA upregulation in response

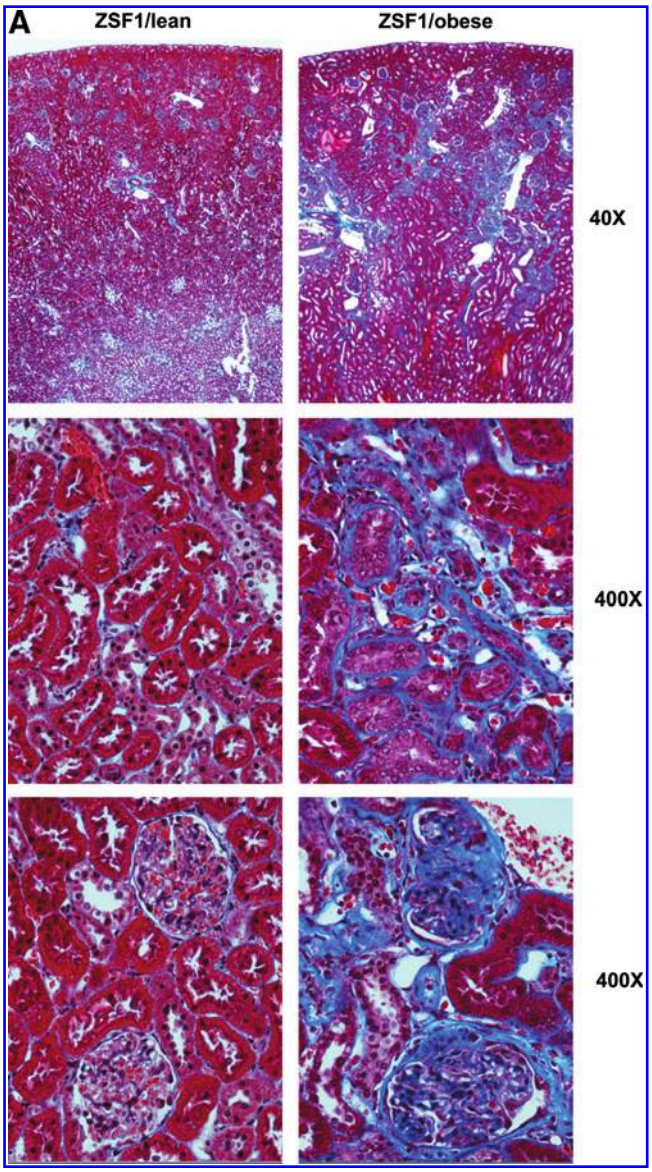

FIG. 2. Tissue was sourced from ZSF1/lean rats (8 weeks old), ZSF1/obese rats (10–35 weeks old). **(A)** Histological staining with Masson's Trichrome on representative ZSF1/lean (8 weeks) and ZSF1/obese (35 weeks) kidneys; **(B)** relative percentages of epithelial (CK8/18/19+), tubular (*GGT1*+), ductular (*AQP2*+), and vascular (*PECAM*+/CD146+) cells in UNFX (passage 0) as measured by flow cytometry; **(C)** relative proportion of UNFX that B2 and B4 represent; **(D)** quantitative flow-cytometric population analysis examining epithelial (*ECAD*/CK8/18/19/PAN-Cadherin), tubular (*GGT1*), ductular (*AQP2*), and vascular (*PECAM*/CD146) marker expression of the B2 subpopulation; and **(E)** qRT-PCR gene expression analysis of B2, expressed relative to B4, for epithelial marker (*ECAD*), tubular marker (*CUB*), glomerular marker (*NEPH*), endocrine marker (*EPO*), and vascular marker *PECAM*.

B

	UNFX yield and flow characterization from rodents with and without CKD	
	ZSF/lean	*ZSF/obese*
Viable cells obtained from tissue (cells/gm $\times 10^6$)	72 ± 32 ($n = 8$)	51 ± 27 ($n = 6$)
CK8/18/19+ (epithelial)	71.5%	60.2%
GGT1+ (tubular)	25.7%	30.6%
AQP2+ (ductular)	40.5%	25.2%

C

	UNFX subpopulation	
	B2 (% of UNFX)	*B4 (% of UNFX)*
ZSF/lean ($n = 2$)	72.0 ± 0.1	3.1 ± 0.1
ZSF1/obese ($n = 1$)	61.3	0.50

D

	B2 flow characterization (% positive)	
	ZSF1/lean	*ZSF1/obese*
Samples assayed	2	1
ECAD	97.6 ± 2.6	93.6
CK8/18/19	99.0 ± 0.3	83.0
GGT1	42.0 ± 5.5	59.6
AQP2	40.0[a]	61.9
PECAM (CD31)	3.0 ± 1.0	1.68

[a] $n = 1$.

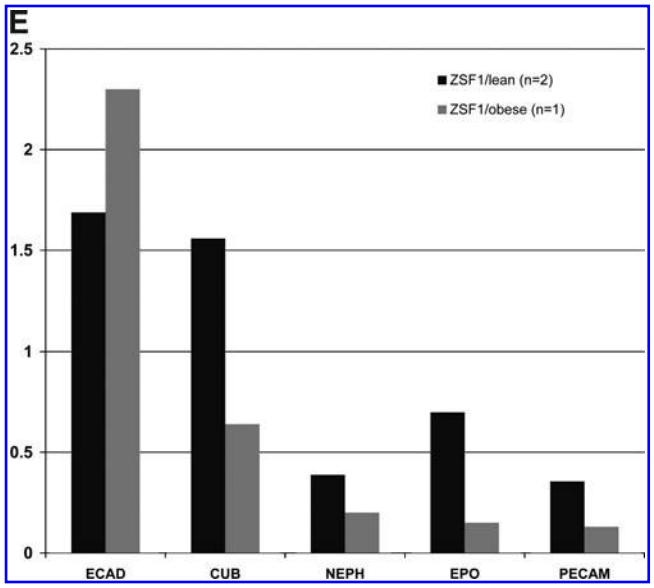

FIG. 2. (Continued).

to hypoxic stimulus was retained in UNFX cultures established from 4/5 CKD and 3/3 non-CKD kidneys (Fig. 4B). In the case of HK022, *EPO* expression was present in the UNFX culture without hypoxia-induced upregulation. UNFX cultures from HK019 failed to express detectable *EPO* mRNA at 21% O_2, but were significantly induced at 2% oxygen. Taken together, these data suggest that cells capable of producing *EPO* are retained in the kidney, even in advanced CKD, and these cells can be isolated and propagated *in vitro* while maintaining oxygen-regulated *EPO*-producing function.

In UNFX cultures from all species, epithelial cells are a predominant phenotype. Functionality of cultured renal tubular cells has been examined historically by a variety of assays, including albumin uptake[20] and the detection of hydrolase activities characteristic of the apical brush border membrane of the renal proximal tubule such as *GGT* and *LAP*.[31,32] These assays were adapted to human UNFX to enable quantitation of albumin uptake and measurement of *GGT* and *LAP* activity and evaluate tubular cell function in UNFX cultures derived from CKD and non-CKD tissue. Regardless of disease state, UNFX cultures retained the functional capacity for protein transport (Fig. 5A–C) and key enzymatic activities involved with proximal tubular cell-specific metabolism (Fig. 5D). Performance of CKD-derived cells was equivalent or superior to non-CKD-derived cells in all three functional assays.

Generation of B2 from biopsy-initiated human UNFX cultures

Clinical scenarios for using an autologous/homologous cell sourcing strategy for CKD therapies have indicated that renal biopsy would be a likely procedure for tissue procurement; therefore, we explored the feasibility of establishing UNFX cultures and B2 subpopulations from tissue harvested with a hollow core device used in clinical practice to collect diagnostic/prognostic biopsies from CKD patients. Population growth of UNFX was examined for 2–4 passages in cultures established from biopsies collected from non-CKD (HK021) or CKD (HK022 and HK023) samples and expansion rates and postculture yields were comparable (Fig. 6A). Because each biopsy of the kidney was taken with a device that permits observation of only the kidney capsule/surface before collection, it was not possible to select areas with healthy tubules or glomeruli; rather, core tissue samples spanning cortex through medulla were collected randomly from different regions of the kidney. Thus, it was of interest to know how reproducible the cellular composition was among biopsies generated from a single kidney.

Six biopsies were obtained from HK022–a CKD kidney–and each biopsy was expanded as an independent UNFX culture. At passage 2, B2 subpopulations were isolated independently from each HK022 UNFX culture and characterized by gene and protein expression profiling to examine reproducibility of the isolation process. Gene expression of the previously identified markers and additional markers were measured in HK022 B2 isolates by quantitative RT-PCR relative to an endogenous control marker (*PPIA*). Genes associated with proximal and distal tubular cells were expressed abundantly in 6/6 of the HK022/B2 replicates with very low variability, indicating the composition of B2 is highly reproducible (Fig. 6B).

A

Human kidney summary characteristics[a]

Sample ID	*Age*	*Gender*	*Disease status*	*Serum creatinine (mg/dL)*
HK16	2 months	F	Non-CKD	0.4
HK17	35 years	F	Non-CKD	2.9
HK18	48 years	F	CKD	8.6
HK19	52 years	F	CKD	5.7
HK20	54 years	F	CKD	16.6
HK21	15 months	M	Non-CKD	0.4
HK22	60 years	M	CKD	3.3
HK23[b]	18 years	M	CKD	6.4

[a]Detailed characteristics of kidneys procured are available online as Supplementary Data.
[b]Obtained as biopsy sample from native kidney by informed consent from patient undergoing kidney transplant.

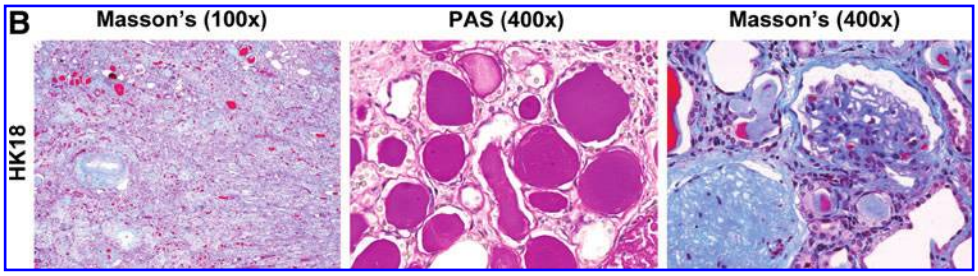

FIG. 3. Human kidney tissue. **(A)** Summary of donor information and disease status of human tissues and **(B)** histopathology of HK18.

Additional studies were conducted to examine reproducibility of the B2 phenotype after serial passage of UNFX. B2 was generated from HK023 UNFX cultures after passage 2 and again after passage 3 and the B2 five-marker protein expression profile was quantitated by flow cytometry (Fig. 6C). As expected, the phenotype of the HK023 B2 subpopulations were >95% epithelial (*ECAD*+ and CK8/18/19+) with a significant proportion of *GGT1*+ tubular cells and a detectable level of *AQP2*+ ductal cells. Trace quantities of *PECAM*+ vascular cells were present as well, but at levels <1%. Interestingly, the percentage of *GGT1*+ and *AQP2*+ cells increased from passage 2 to passage 3, suggesting that key epithelial cell types characteristic of B2 are retained during UNFX subculture.

Discussion

Currently, a defined regulatory approval pathway exists to move regenerative medicine therapies that incorporate cells sourced via an autologous/homologous strategy into clinics.[6–8] Although numerous practical challenges are inherent to developing and delivering therapies that incorporate autologous cells, autologous approaches remain attractive clinically because they avoid the need for immune suppression and may circumvent some concerns regarding pathogens. However, autologous/homologous sourcing strategies may prove infeasible when cell(s) of therapeutic interest are not procurable from the organ of interest in the target patient population due to disease-related destruction (e.g., insulin-producing beta cells in type 1 diabetes mellitus) or because of clinical risk associated with direct sourcing. Such limitations have led some to procure therapeutically relevant cells from an ectopic site, also known as an "autologous/heterologous cell sourcing strategy,"[6] or to employ stem or multilineage cells. When the therapeutically relevant cells are highly specialized, tissue-specific cells, these alternative approaches may face additional development challenges (e.g., difficulty scaling-up due to inefficiencies of differentiation protocols, and need to assess long-term stability of differentiated phenotype).[33] Studies in both the liver and kidney have indicated that resident parenchymal cells are more efficient than ectopically derived stem and progenitor cells at restoring function to damaged tissue after injury.[15,34,35] These factors guided our decision to evaluate the feasibility of ICE defined renal subpopulations from CKD-relevant animal models and from diseased kidney tissue in humans.

Methods for isolating UNFX and the subpopulations obtained from UNFX by density gradient centrifugation were translated to two CKD-relevant animal models: ZSF1 (*fa*/*fa*^{cp}) rat and dog. The ZSF1(*fa*/*fa*^{cp}) rat provides a model of renal failure secondary to obesity and insulin-resistant diabetes, and thus potentially represents a major portion of the CKD population worldwide.[1,36,37] The obese ZSF1 model is characterized by age-dependent progressive nephropathy,[29] with systemically measurable renal degeneration (e.g., elevated BUN, sCREAT, and proteinuria). In a veterinary setting, aged dogs often present with spontaneously occurring chronic renal failure, the symptoms and progressive nature of which mimic key elements of CKD in humans.[38] Consequently, the dog is frequently selected as a preclinical

Table 4. Summary Comparison of Human Samples by Disease Status

			Comparison of human samples by disease status	
			Nonchronic kidney disease	*Chronic kidney disease*
B2 isolating, characterizing, and expanding characteristics	UNFX isolating, characterizing, and expanding characteristics		Viable cells obtained from tissue [(cells/gm) $\times 10^6$]	26 ± 24	9 ± 7
			Doubling time in culture (hours)	19.4	22.8
			Hypoxic induction of *EPO* (2% O2: 21% O2 expression ratio)	1.6 ± 1.0	3.3 ± 1.0
			Receptor-mediated albumin uptake (% ALB-*RHO*-positive cells)	48.0	67.3
			LAP activity (index value)	28.8 ± 0.1	28.0 ± 0.5
			GGT activity (index value)	8.1 ± 0.2	13.1 ± 0.2
	Density gradient yields		B2 subpopulation (% of UNFX)	49	50.5 ± 0.2
			B4 subpopulation (% of UNFX)	2.7	1.9 ± 0.02
			CK8/18/19 (epithelial) (% positive by flow cytometry)	99.1 ± 0.6	98.9 ± 0.2
	Gene Expression Relative to B4	Protein Expression	*GGT1* (renal tubule) (% positive by flow cytometry)	51.5 ± 4.0	47.9 ± 29
			AQP2 (collecting duct) (% positive by flow cytometry)	41.1	38.7 ± 19
			ECAD (distal tubule) (B2:B4 expression ratio)	0.78	2.41
			CUB (proximal tubule) (B2:B4 expression ratio)	1.45	1.14
			NEPH (glomerular) (B2:B4 expression ratio)	0.12	0.58
			EPO (endocrine) (B2:B4 expression ratio)	0.65	0.55
			PECAM (endothelial) (B2:B4 expression ratio)	0.02	0.06

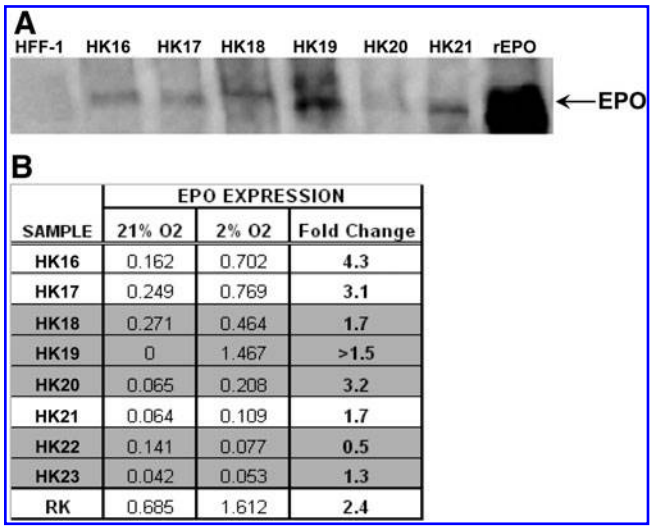

SAMPLE	EPO EXPRESSION 21% O2	2% O2	Fold Change
HK16	0.162	0.702	4.3
HK17	0.249	0.769	3.1
HK18	0.271	0.464	1.7
HK19	0	1.467	>1.5
HK20	0.065	0.208	3.2
HK21	0.064	0.109	1.7
HK22	0.141	0.077	0.5
HK23	0.042	0.053	1.3
RK	0.685	1.612	2.4

FIG. 4. **(A)** Expression of *EPO* protein was examined in whole kidney tissue from three nonchronic kidney disease (CKD) human specimens (HK16, HK17, and HK21) and three CKD human specimens (HK18, HK19, and HK20); specificity was achieved by separating proteins by isoelectric focusing and detection with monoclonal antibody. Human foreskin fibroblasts (HFF-1) and recombinant human *EPO* protein (rEPO) were used as negative and positive controls, respectively. **(B)** *EPO* gene expression in passage 1 and passage 2 UNFX cultures established from human tissues at 24 h in 21% oxygen or 2% oxygen before harvest. Rat kidney (RK) UNFX cultures at passage 0 served as a positive control. Fold change was calculated by dividing expression at 2% oxygen by expression at 21% oxygen.

model of kidney disease in the laboratory setting, where surgery, ischemia, and/or chemical treatment are used to achieve reduction in functional nephron mass.[39–41]

Demonstrating feasibility for autologous cell sourcing in disease-relevant animal models is necessary, but not sufficient, for translating product development into clinics; therefore, ICE methods were also evaluated with healthy and diseased human kidney tissues. In addition, the sampling methods used to obtain tissue from diseased kidneys (e.g., needle biopsy) replicated tissue sampling practices used in the clinic to obtain diagnostic biopsies.[42] The preliminary data obtained in this study on the isolation, characterization, and expansion of UNFX and UNFX-derived subpopulations will be valuable for guiding the design of future experiments as more information becomes available regarding the number and type(s) of cells needed to achieve a therapeutically relevant outcome.

The presence and function of specific kidney cell types (e.g., tubular cells and *EPO*-producing cells) were investigated in UNFX and B2 cultures established and propagated from rodents, dogs, and humans, including rodents and humans with confirmed CKD. Despite lower initial cell yields from CKD versus non-CKD kidney tissues, growth rates and population doubling times were comparable (Table 4 and Fig. 6). This study demonstrated that tubular cells are major components of UNFX cultures across species and disease states and are further enriched in the B2 subpopulation generated by density gradient centrifugation. In addition to the tubular phenotypic reproducibility measured by gene expression and flow cytometry, key tubule-associated functions such as receptor-mediated albumin transport and hydrolase activities involved in metabolism (*GGT* and *LAP*) were retained in B2. Functional attributes of the tubular cells present in CKD-derived cultures were comparable or superior to non-CKD-derived cultures (summarized in Table 4), despite significant systemic and histologic disease of the kidneys at the time of tissue procurement, suggesting that

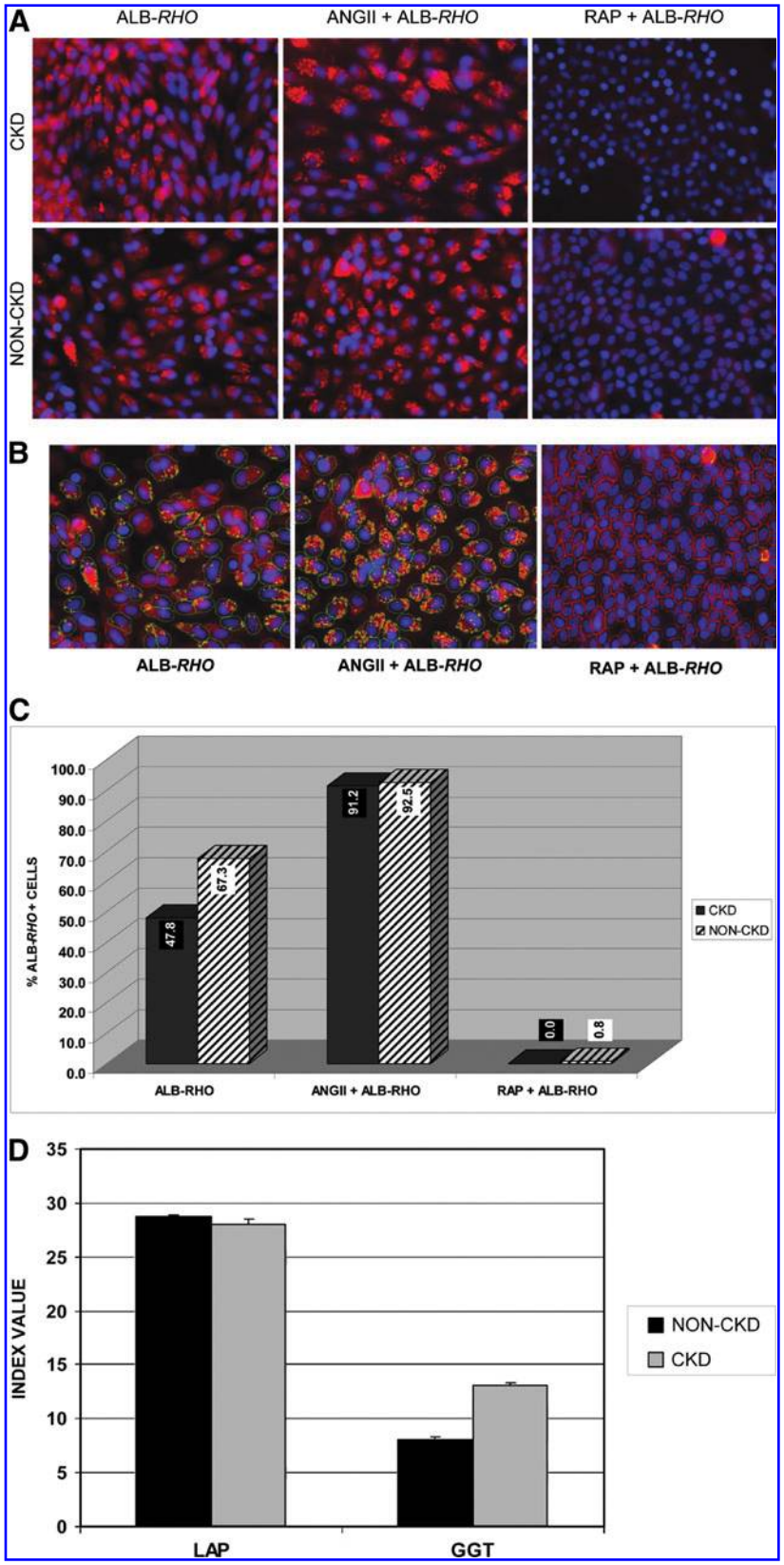

FIG. 5. Functional attributes of human UNFX cultures (passage 1) derived from non-CKD (HK21) and CKD (HK22) kidneys. **(A)** Protein transport function as measured by uptake of rhodamine-conjugated albumin (ALB-*RHO*). Specificity of the reaction was confirmed by enhanced uptake of ALB-*RHO* in the presence of angiotensin II (ANGII), and by blockage of ALB-*RHO* uptake in the presence of receptor-associated protein (RAP), a competitive inhibitor of receptor-mediated albumin transport. **(B)** Quantitation of cells positive for ALB-*RHO* uptake (green outline) counted with IN Cell Investigator Software with Multi-Target Analysis Module. Analyzed images with masks applied are shown for HK21. **(C)** Relative percentages of ALB-*RHO*(+) cells after exposure to *RHO*-ALB, ANGII + ALB-*RHO*, and RAP + ALB-*RHO*. **(D)** Quantitation of leucine aminopeptidase (*LAP*) and gamma glutamyl transferase (*GGT*) enzymatic activities.

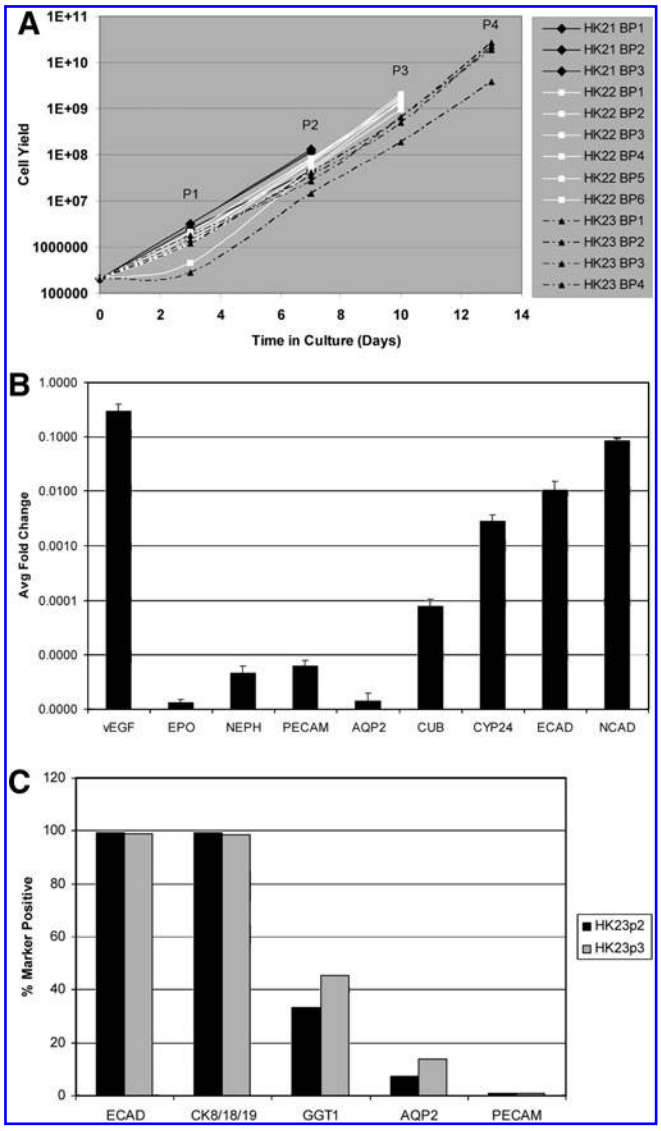

FIG. 6. Reproducibility of core needle biopsy punch sourcing of UNFX and B2 from non-CKD (HK21) and CKD (HK22 and HK23) kidneys. UNFX cultures were harvested and subcultured (passaged) 2–4 times and quantified with each passage. **(A)** Growth rates of UNFX cultures generated from biopsies of HK21 ($n = 3$, solid black lines), HK22 ($n = 6$, white lines), and HK23 ($n = 4$, dotted black lines). **(B)** Passage 2 UNFX cultures, established separately from each of the six HK22 biopsies, were used to generate B2 subfractions. Expression of tubular (vascular endothelial growth factor VEGF, *CUB*, *CYP24*, *ECAD*, and *NCAD*), ductular (*AQP2*), glomerular (*NEPH*), vascular (*PECAM*), and endocrine (*EPO*) markers were measured by quantitative RT-PCR and calibrated to an endogenous control (peptidylprolyl isomerase A) (shown as mean ± standard deviation). **(C)** Phenotypic fidelity of B2 subfractions generated from an HK23 biopsy at passages 2 and 3 by flow cytometry for epithelial (CK8/18/19), tubular (*ECAD*, *GGT1*), ductular (*AQP2*), and vascular (*PECAM*) markers.

cells with therapeutic potential can be sourced by an autologous/homologous strategy from severely diseased tissue, even though such functions are compromised *in situ*. The ICE methods evaluated in this study reproducibly generated B2, a renal cell subpopulation enriched in functional tubular cell components and relatively depleted of other cell types, including large collecting duct cells, glomerular cells, endocrine cells, and vascular cells. Such phenotypic and functional reproducibility is compatible with the requirements of clinical manufacturing.

The *EPO*-producing cells of the kidney have been isolated and described as components of heterogeneous primary renal cell cultures.[9,26] In the present study, *EPO*-producing cells were identified in UNFX cultures derived from rodent, dog, and human. *EPO*-producing cells were also present in UNFX cultures isolated from CKD tissue. In all cases tested, *EPO* expression was oxygen regulated; exposure of UNFX cultures to low (2%) oxygen levels increased *EPO* expression significantly compared to atmospheric (21%) oxygen. Multiple mechanisms have been hypothesized as explanations for anemia secondary to CKD; however, there is general agreement that *EPO* deficiency plays a role, as serum *EPO* levels are decreased in human CKD patients in proportion to the degree of anemia.[43] Some have postulated that *EPO*-producing cells are lost from the kidney as CKD progresses; our data provide evidence against a complete loss of *EPO*-producing cell mass, as four of five CKD kidneys and the UNFX cultures derived from these organs contained *EPO*-producing cells. During density gradient centrifugation of UNFX isolates, *EPO*-producing cells, along with glomerular and vascular cells become enriched in the B4 fraction in all species (Fig. 2B). Given the potential therapeutic value of oxygen-regulated *EPO*-producing cells,[44] it may be beneficial to investigate the therapeutic benefit of administering B4 alone or in controlled admixtures with other renal subpopulations in future *in vivo* experiments.

Of importance to tissue engineering is the expansion capacity of the input cultures from which therapeutically relevant cells are produced.[45] Ongoing studies are investigating the therapeutic potential of UNFX and the cell subpopulations described in this report; however, the focus of these studies was to investigate the feasibility of generating the cellular component of an autologous treatment for CKD from animal models relevant for product prototype evaluation and from diseased human kidneys. The initial yields of viable cells from tissues are presented for all species studied and data on the expansion capacity of human UNFX cultures derived from non-CKD and CKD tissues are presented in Figure 6. Although evaluations of optimal and maximal expansion parameters must await the identification and characterization of therapeutically relevant cell populations and dose ranges, Figure 6 illustrates consistency in UNFX expansion and presents growth rate data that is relevant for a preliminary assessment of feasibility. For example, the growth rates of four replicate UNFX cultures derived from HK23 (obtained from a CKD patient with serum creatinine of 6.4) did not yet exhibit a plateau at passage 4 (P4) and the cell yield of three out of four replicate cultures was $>1 \times 10^{10}$ cells. If a therapeutically relevant subpopulation was present at only 1% of UNFX, this yield would still represent 1×10^{8}, or 100 million cells. Such a yield, obtained without optimization of cell culture conditions, falls within a dose range that elicited *de novo* regeneration of urinary tissue in animals.[46,47] B2, the tubular-enriched UNFX subpopulation B2, which previous studies suggest might have therapeutic potential based on its tubular-enriched composition,[12–16] represents on average 50% of UNFX. Again, the yield of B2 that could be isolated from a

UNFX culture derived from a biopsy sample of CKD tissue at <14 days in culture (HK23 at P4) is $>5 \times 10^9$ B2 cells, a yield that falls within or exceeds dose ranges that elicited *de novo* urinary tissue regeneration in animals.[46,47]

In summary, these studies demonstrate that primary cultures containing cells from all major compartments of the kidney (UNFX) and two subpopulations whose compositions are each suggestive of potential therapeutic value[12–16,44]—a tubular cell-enriched subpopulation (B2) and a subpopulation containing oxygen-responsive Epo-producing cells (B4)—can be established reproducibly from healthy and diseased kidney tissue across multiple species. The successful adaptation of ICE methods to large animal and human CKD specimens highlights the feasibility of pursuing an autologous/homologous cell sourcing strategy for obtaining the cellular component of candidate regenerative therapies for CKD and translating such candidate therapies from preclinical to clinical evaluation. Despite advanced fibrosis and complex underlying metabolic disease, pockets of tubular, endocrine, collecting duct, and glomerular cells persist within CKD-derived tissue, providing access to the building blocks that may be required components of an autologous regenerative medicine therapy with the potential to preserve renal function and extend lifespan in many patients with CKD.

Disclosure Statement

All authors are employees of Tengion or were employees when experiments were performed.

References

1. U.S. Renal Data System. Costs of CKD and ESRD. Minneapolis, MN, 2007.
2. Annual Report of the U.S. Organ Procurement and Transplantation Network and the Scientific Registry of Transplant Recipients: Transplant Data 1998–2007. Rockville, MD: HHS/HRSA/HSB/DOT, 2008.
3. Wolfe, R.A., Ashby, V.B., Milford, E.L., Ojo, A.O., Ettenger, R.E., Agodoa, L.Y., *et al.* Comparison of mortality in all patients on dialysis, patients on dialysis awaiting transplantation, and recipients of a first cadaveric transplant. N Engl J Med **341,** 1725, 1999.
4. Laupacis, A., Keown, P., Pus, N., Krueger, H., Ferguson, B., Wong, C., *et al.* A study of the quality of life and cost-utility of renal transplantation. Kidney Int **50,** 235, 1996.
5. Magee, C.C., and Pascual M. Update in renal transplantation. Arch Intern Med **164,** 1373, 2004.
6. Bertram, T.A., and Jayo, M.J. Tissue engineered products: preclinical development of neo-organs. In: Cavagnero, J., ed. Preclinical Safety Evaluation of Biopharmaceuticals: A Science-Based Approach to Facilitating Clinical Trials. New York: John Wiley & Sons, 2008. pp. 799–826.
7. ClinicalTrials.gov. Augmentation Cystoplasty Using an Autologous Neo-Bladder. ClinicalTrials.gov, 2010.
8. ClinicalTrials.gov. Study of Autologous Neo-Bladder Construct in Subjects with Neurogenic Bladder Following Spinal Cord Injury. ClinicalTrials.gov, 2010.
9. Aboushwareb, T., Egydio, F., Straker, L., Gyabaah, K., Atala, A., and Yoo, J.J. Erythropoietin producing cells for potential cell therapy. World J Urol **26,** 295, 2008.
10. Joraku, A., Stern, K.A., Atala, A., and Yoo, J.J. *In vitro* generation of three-dimensional renal structures. Methods **47,** 129, 2009.
11. Kirpatovskii, V.I., Kazachenko, A.V., Plotnikov, E.Y., Marei, M.V., Musina, R.A., Nadtochii, O.N., *et al.* Experimental intravenous cell therapy of acute and chronic renal failure. Bull Exp Biol Med **143,** 160, 2007.
12. Bonventre, J.V. Dedifferentiation and proliferation of surviving epithelial cells in acute renal failure. J Am Soc Nephrol **14 Suppl 1,** S55, 2003.
13. Duffield, J.S., and Bonventre, J.V. Kidney tubular epithelium is restored without replacement with bone marrow-derived cells during repair after ischemic injury. Kidney Int **68,** 1956, 2005.
14. Duffield, J.S., Park, K.M., Hsiao, L.L., Kelley, V.R., Scadden, D.T., Ichimura, T., *et al.* Restoration of tubular epithelial cells during repair of the postischemic kidney occurs independently of bone marrow-derived stem cells. J Clin Invest **115,** 1743, 2005.
15. Held, P.K., Al-Dhalimy, M., Willenbring, H., Akkari, Y., Jiang, S., Torimaru, Y., *et al. In vivo* genetic selection of renal proximal tubules. Mol Ther **13,** 49, 2006.
16. Tumlin, J., Wali, R., Williams, W., Murray, P., Tolwani, A.J., Vinnikova, A.K., *et al.* Efficacy and safety of renal tubule cell therapy for acute renal failure. J Am Soc Nephrol **19,** 1034, 2008.
17. Griffin, K.A., Abu-Naser, M., Abu-Amarah, I., Picken, M., Williamson, G.A., and Bidani, A.K. Dynamic blood pressure load and nephropathy in the ZSF1 (fa/fa cp) model of type 2 diabetes. Am J Physiol Renal Physiol **293,** F1605, 2007.
18. Ausabel, F.M., Brent, R., Kingston, R.E., Moore, D.D., Seidman, J.G., Smith, J.A., *et al.* Current Protocols in Molecular Biology. Somerset, NJ: John Wiley & Sons, 2010.
19. Ormerod, M.G. Flow Cytometry: A Practical Approach. New York: Oxford University Press, 2000.
20. Zhai, X.Y., Nielsen, R., Birn, H., Drumm, K., Mildenberger, S., Freudinger, R., *et al.* Cubilin- and megalin-mediated uptake of albumin in cultured proximal tubule cells of opossum kidney. Kidney Int **58,** 1523, 2000.
21. Caruso-Neves, C., Kwon, S.H., and Guggino, W.B. Albumin endocytosis in proximal tubule cells is modulated by angiotensin II through an AT2 receptor-mediated protein kinase B activation. Proc Natl Acad Sci USA **102,** 17513, 2005.
22. Tate, S.S., and Meister, A. Gamma-glutamyl transpeptidase from kidney. Methods Enzymol **113,** 400, 1985.
23. Chung, S.D., Alavi, N., Livingston, D., Hiller, S., and Taub, M. Characterization of primary rabbit kidney cultures that express proximal tubule functions in a hormonally defined medium. J Cell Biol **95,** 118, 1982.
24. Prophet, E.B., Mills, B., Arrington, J.B., and Sobin, L.H. Armed Forces Institute of Pathology: Laboratory Methods in Histotechnology. Washington, DC: American Registry of Pathology, 1992.
25. Shackelford, C., Long, G., Wolf, J., Okerberg, C., and Herbert, R. Qualitative and quantitative analysis of nonneoplastic lesions in toxicology studies. Toxicol Pathol **30,** 93, 2002.
26. Presnell, S., Bruce, A., Wallace, S., Choudhury, S., Kelley, R., Tatsumi, P., *et al.* Isolation and characterization of bioresponsive renal cells from human and large mammal with chronic renal failure. FASEB J **23,** LB143, 2009.
27. Bruce, A.T., Sangha, N., Richmond, A., Johnson, K., Jones, S., Spencer, T., *et al.* Use of iodixanol self-generated density gradients to enrich for viable urothelial cells from nonneurogenic and neurogenic bladder tissue. Tissue Eng Part C Methods **16,** 33, 2010.

28. Dominguez, J.H., Wu, P., Hawes, J.W., Deeg, M., Walsh, J., Packer, S.C., *et al.* Renal injury: similarities and differences in male and female rats with the metabolic syndrome. Kidney Int **69,** 1969, 2006.
29. Prabhakar, S., Starnes, J., Shi, S., Lonis, B., and Tran, R. Diabetic nephropathy is associated with oxidative stress and decreased renal nitric oxide production. J Am Soc Nephrol **18,** 2945, 2007.
30. Tofovic, S.P., Kusaka, H., Kost, C.K., Jr., and Bastacky, S. Renal function and structure in diabetic, hypertensive, obese ZDFxSHHF-hybrid rats. Ren Fail **22,** 387, 2000.
31. Ryan, M.J., Johnson, G., Kirk, J., Fuerstenberg, S.M., Zager, R.A., and Torok-Storb, B. HK-2: an immortalized proximal tubule epithelial cell line from normal adult human kidney. Kidney Int **45,** 48, 1994.
32. Yang, A.H., Gould-Kostka, J., and Oberley, T.D. *In vitro* growth and differentiation of human kidney tubular cells on a basement membrane substrate. In Vitro Cell Dev Biol **23,** 34, 1987.
33. Hentze, H., Soong, P.L., Wang, S.T., Phillips, B.W., Putti, T.C., and Dunn, N.R. Teratoma formation by human embryonic stem cells: evaluation of essential parameters for future safety studies. Stem Cell Res 2009 [Epub ahead of print].
34. Guo, J.K., and Cantley, L.G. Cellular maintenance and repair of the kidney. Annu Rev Physiol **72,** 357, 2010.
35. Overturf, K., Al-Dhalimy, M., Finegold, M., and Grompe, M. The repopulation potential of hepatocyte populations differing in size and prior mitotic expansion. Am J Pathol **155,** 2135, 1999.
36. Eknoyan, G. Obesity, diabetes, and chronic kidney disease. Curr Diabetes Rep **7,** 449, 2007.
37. Hsu, C.Y., Iribarren, C., McCulloch, C.E., Darbinian, J., and Go, A.S. Risk factors for end-stage renal disease: 25-year follow-up. Arch Intern Med **169,** 342, 2009.
38. Krawiec, D.R. Urologic disorders of the geriatric dog. Vet Clin North Am Small Anim Pract **19,** 75, 1989.
39. Finco, D.R., Brown, S.A., Brown, C.A., Crowell, W.A., Cooper, T.A., and Barsanti, J.A. Progression of chronic renal disease in the dog. J Vet Intern Med **13,** 516, 1999.
40. Fine, A., Jones, D., Kaushal, G., LeGal, Y., and Sharma, G. Remnant model of renal failure in the dog: avoidance of second surgery by chemical nephrectomy. Clin Invest Med **13,** 152, 1990.
41. Hall, J.E., Mizelle, H.L., Brands, M.W., and Hildebrandt, D.A. Pressure natriuresis and angiotensin II in reduced kidney mass, salt-induced hypertension. Am J Physiol **262,** R61, 1992.
42. Whittier, W.L., and Korbet, S.M. Renal biopsy: update. Curr Opin Nephrol Hypertens **13,** 661, 2004.
43. Nangaku, M., and Eckardt, K.U. Pathogenesis of renal anemia. Semin Nephrol **26,** 261, 2006.
44. Jelkmann, W. Control of erythropoietin gene expression and its use in medicine. Methods Enzymol **435,** 179, 2007.
45. Lanza, R., Langer, R., and Vacanti, C.A. Principles of Tissue Engineering. Burlington, MA: Elsevier Academic Press, 2008.
46. Jayo, M.J., Jain, D., Ludlow, J.W., Payne, R., Wagner, B.J., McLorie, G., *et al.* Long-term durability, tissue regeneration and neo-organ growth during skeletal maturation with a neo-bladder augmentation construct. Regen Med **3,** 671, 2008.
47. Jayo, M.J., Jain, D., Wagner, B.J., and Bertram, T.A. Early cellular and stromal responses in the regeneration of a functional mammalian bladder. J Urol **180,** 392, 2008.

Address correspondence to:
Sharon C. Presnell, Ph.D.
Tengion Laboratories
Department of Science and Technology
3929 Westpoint Blvd., Suite G
Winston-Salem, NC 27103

E-mail: sharon.presnell@tengion.com

Received: July 7, 2010
Accepted: September 15, 2010
Online Publication Date: October 22, 2010

This article has been cited by:

1. Christopher W. Genheimer, Roger M. Ilagan, Thomas Spencer, Rusty W. Kelley, Eric Werdin, Sumana Choudhury, Deepak Jain, John W. Ludlow, Joydeep Basu. 2012. Molecular Characterization of the Regenerative Response Induced by Intrarenal Transplantation of Selected Renal Cells in a Rodent Model of Chronic Kidney Disease. *Cells Tissues Organs* **196**:4, 374-384. [CrossRef]